Cellulosic Fiber: Mechanical Fibrillation-Morphology-Rheology Relationships

Tianzhong Yuan
South China University of Technology
Jinsong Zeng (fezengjs@scut.edu.cn)
South China University of Technology https://orcid.org/0000-0002-0335-3405
Bin Wang
South China University of Technology
Zheng Cheng
South China University of Technology
Kefu Chen
South China University of Technology

Research Article

Keywords: cellulosic fiber, morphological properties, mechanical fibrillation, rheological behavior

Posted Date: May 21st, 2021

DOI: https://doi.org/10.21203/rs.3.rs-469007/v1

Version of Record: A version of this preprint was published at Cellulose on July 6th, 2021. See the published version at https://doi.org/10.1007/s10570-021-04034-y.

Abstract

This study aims to investigate the relationship between mechanical fibrillation, morphological properties, and rheological behavior of cellulosic fiber. Three types of cellulosic fibers were obtained by adjusting mechanical fibrillation, namely squashed cellulose, incompletely nanofibrillated cellulose, and completely nanofibrillated cellulose, respectively. The squashed cellulose with large size and small aspect ratio had low entanglement capacity, thus forming a weak fiber network. The corresponding suspension exhibited low viscosity, weak elastic behavior, small yield stress, and low dynamic stability. An obviously increasing aspect ratio and entanglement capacity were observed with increasing mechanical fibrillation, resulting in entangled fiber network structure. Hence, the cellulosic fiber suspension obtained by more mechanical fibrillation exhibited higher viscosity, stronger gel-like behavior, and bigger yield stress. Moreover, the extremely entangled fiber network structure has better anti-deformation capacity and recovery capacity. We revealed the fundamental insights into the relationship between morphologies and rheological properties of cellulosic fiber, paving the way for designing cellulose-based materials.

Introduction

Nanofibrillated cellulose, the class of cellulosic nanomaterials, attracted growing interest due to their excellent mechanical properties, large aspect ratio, biodegradable nature, low density, and renewability (Abdul Khalil et al. 2014; Habibi 2014; Mendoza et al. 2019; Phanthong et al. 2018; Tian et al. 2019). It has shown promising results for the production of nanocomposite materials including paper additives, reinforcements for polymer composites, drug carriers, antibacterial materials, emulsions, conductive materials (Bai et al. 2018; Chen et al. 2020; Gómez H. et al. 2016; Grishkewich et al. 2017; Hoeng et al. 2017; Kedzior et al. 2020; Yuan et al. 2021). In general, nanofibrillated cellulose is mainly produced by mechanical disintegration, which has a diameter of nanoscale and length of micrometer scale (Nechyporchuk et al. 2016; Zhuo et al. 2017). In this process, the hydrogen bond and cell wall structure of cellulose were broken down by shear forces leading to the cellulose fibrillation. At the same time, mechanical fibrillation produced the strongly aggregated and twisted fibers and highly entangled fiber network (Albornoz-Palma et al. 2020; Nechyporchuk et al. 2016; Yuan et al. 2021). Consequently, the morphological properties and the size of nanofibrillated cellulose were extremely complicated.

Generally, the morphological properties of fiber and fiber network structure of cellulosic fiber suspensions are closely correlative with the rheological properties (Czaikoski et al. 2020; Karppinen et al. 2011; Moon et al. 2011). The unique morphological properties and concentration of fibers can create a unique fiber structure in cellulosic fiber suspension, which display the corresponding viscosity, viscoelastic property, anti-formation ability, and the dynamic stability. Rheology is the study of flow and deformation of matter under the influence of an applied force as a function of time, which can reflect the relationship between the strength of internal structure and the external force (Karato and Wu 1993; Sun et al. 2017; Taheri and Samyn 2016; Wang et al. 2020; Xu et al. 2017). Therefore, rheological behavior helps to precisely reveal the dispersion microstructure of the cellulose-based suspensions (Li et al. 2015; Quennouz et al. 2016; Yadav et al. 2021). Moreover, cellulosic fiber has the excellent self-assemble ability, which can reconstruct

a new fiber network structure when the original structure was breakdown. Rheological properties are fundamental to understand the assembly mechanism and the process of reconstructed fiber structure (Derakhshandeh et al. 2010; Dimic-Misic et al. 2013; Iotti et al. 2011; Peng et al. 2018). Although numerous mechanical methods for creating nanofibrillated cellulose have been reported in early studies, only a few researches studied on the rheological properties of cellulosic fiber suspensions, much less on the effect of morphological properties on the rheological behavior. These studies mainly discussed the controlling factors for the rheological behavior of cellulosic fiber suspensions, for example, the shear viscosity and the viscoelastic properties for various concentration of cellulosic fiber suspension (Alves et al. 2020; Chen et al. 2013), the rheological difference between cellulose nanocrystals and cellulose nanofibers (Li et al. 2015), the effect of ion and surface characteristics on the rheology of cellulose nanocrystals (Jiang et al. 2020; Moberg et al. 2017; Xu et al. 2019, 2020), and rheological modifiers, foodstuff, related cosmetic and biomedical applications (Dhand et al. 2021; Dinic and Sharma 2020; Espert et al. 2020; Heggset et al. 2020; Jiang et al. 2017). However, there were few reports about the relationship between morphological change of cellulosic fiber and the rheological properties of cellulosic fiber suspension (Li et al. 2015; Lindström 2017; Taheri and Samyn 2016). Importantly, morphological properties of cellulose have a significant effect on viscoelastic behavior, creep and strain recovery, recovery capability after disruption, and apparent yield stress, which have not yet been detailed. The purpose of the present study is to gain further understanding the effect of intricate cellulosic fiber morphology on rheological behavior. Subsequently, good sight in the relationships between mechanical fibrillation, morphological properties and rheological properties of cellulosic fiber suspensions should be established.

In this study, cellulosic fiber with different size and morphological properties was obtained by adjusting mechanical fibrillation. The effect of morphological properties on the rheological properties of cellulosic fiber suspensions were characterized by viscosity, viscoelastic properteis, shear-thinning behavior. The creep compliance and apparent yield stress were further detailed, which will contribute to the better understanding of anti-deformation capacity and strength of fiber network structure formed by different morphologies. It is desired that a deeper comprehension of these relationships can provide us more practical guidance on the development of cellulosic fiber-based materials with finely controlled properties.

Materials And Methods

Materials

The raw material was Bleached-Chemi-Thermo-Mechanical-Pulp from UPM (Maple 80, Changshu, China).

Chemical compositions of material

The chemical constituents of pulp were tested by acid hydrolysis (Bian et al. 2019). Firstly, the pulp was hydrolyzed in 72 wt.% sulfuric acid at 30°C for 1 h. The second step was hydrolyzed in 4 wt.% sulfuric acid at 121°C for 1 h. The ion chromatography was carried out for carbohydrate analysis. The residue was detected by gravimetrically the klason lignin contents. Consequently, BCTMP as raw material

contains klason lignin of 2.43%, glucan of 80.14%, xylan of 9.43%, mannan of 5.73%, galactan of 1.52%, and arabanan of 0.75%.

Preparation of cellulosic fiber

The pulp with 1 wt.% concentration was disintegrated using Valley Beaters with 1h (PL4-2 Xianyang Test Equipment Co., LTD, China). And mechanical fibrillation of obtained suspension was performed by SuperMassColloider under the disks gap of -100 μm at 2000 rpm (MKCA62 J Masuko Sangyo Co., LTD, Japan). Sample grinded after 10 times was named as A10, and that after 20 times and 40 times were named A20 and A40, respectively.

Morphological properties of cellulosic fiber

Morphological properties of obtained cellulosic fiber were tested by atomic force microscopy (AFM, Bruker, Germany) and field-emission scanning electron microscopy (FE-SEM Merlin, Zeiss, Germany). Firstly, the cellulosic fiber suspension with 0.01 wt.% was dispersed by sonication treatment. Then, the cellulosic fiber droplet was dropped on the surface of clear mica pieces. The AFM test was operated after air drying. In addition, the sample was sputtered with gold before SEM test. The length and diameter were analyzed by ImageJ (Version 1.49) as shown in Table 1.

Table 1
Calculated parameters for obtained cellulose

Sample	Times of mechanical fibrillation	Morphologies of cellulose	Crystallinity index (%)	Diameter (μm)	Length (μm)	Aspect ratio
A10	10	Squashed	60.76	15.49	217.49	14.04
A20	20	Incompletely nanofibrillated	56.29	0.41	11.43	27.88
A40	40	Completely nanofibrillated	47.65	0.12	9.93	82.75

Rheological Measurements of cellulosic fiber suspension

The cellulosic fiber suspensions with different concentration were prepared and their rheological behavior was detected by a stress-controlled rheometer (DHR-3, TA instrument, Inc., USA) using a plate geometry with diameter of 40 mm. The viscosity was tested in rang of shear rates from 0.01 to 1000 s^{-1} at 25°C. The viscoelastic responses, including the storage modulus (G') and the loss modulus (G''), were detected via oscillatory mode. The strain sweeps were carried out for the linear viscoelastic region within the strain from 0.01 to 1000% under the frequency of 1.0 Hz. And frequency sweeps were performed with frequency from 0.1 to 100 rad/s within the linear viscoelastic region. Two types of shear modes, small amplitude oscillatory shear with the strain level of 0.1% and large amplitude oscillatory shear one with 500% strain, were tested by oscillatory mode. The compliance of cellulosic fiber suspension was operated by step

creep with 300s under shear stresses of 0.3 Pa, and unloading of stress with 900s. The influence of temperature on viscosity was tested with temperature from 20°C to 90°C at a constant shear rate of 0.1 s^{-1}. The yield stress values of the cellulosic fiber suspension were performed by following method (Derakhshandeh et al. 2010). The step creep tests were done at the increasing shear stress over a time of 300 s. The yield stress was measured as the minimum stress value which can drive the suspension to flow.

Results And Discussion

Morphological properties of cellulosic fibers

The morphological properties of cellulosic fibers obtained after grinding with different times were characterized using SEM and AFM as shown in Fig. 1 and Fig. 2. After ten times of grinding treatment (sample A10), the cylindrical and bunchy original cellulose fibrils were squashed under the shear force when the pulp slurry passed the gap between the static and rotating grind stone. A few individual nanofibrillated cellulose were found at the ends and edges of the squashed cellulose. But the vast majority of fibrils were still tightly aligned along the cellulose and closely connected to each other with the ‘band’ feature. It suggested that ten times of grinding treatment can’t completely break down the hydrogen bonds and cell wall structures. The size of sample A10 was basically kept at the micrometer in diameter, as shown in Table 1. After 20 times of grinding treatments, the size of cellulosic fiber was obviously decreased due to the partial breakage of hydrogen bonds and cell wall structures. As shown in Fig. 1d-f, the internal fibrillation of cellulose increased with increasing the times of grinding treatment, thus presenting a ‘tree’ feature. A mass of nanofibrillated individual cellulose appeared at the ends of squashed cellulose like the branches of trees (Fig. 2f), ranging from the large nano-size of several hundred nanometers to the small nano-size of about a few nanometers. It suggested that the amount of fibrillation was obviously improved with increasing mechanical fibrillation. But the center section of squashed cellulose with approximately several micrometers was a non-individual body like the ‘tree trunk’. Similar morphological properties have been reported in other studies (Phanthong et al. 2018; Wang et al. 2016). After 40 times of grinding treatments, most part of cellulose was completely nanofibrillated producing the long and flexible nanofibrillated cellulose with tens of nanometer in diameter. No obvious center ‘tree trunk’ sections were retained, implying the hydrogen bonds and cell wall structures were entirely broken down. As a result, the amount of fibrillation was increased and size in diameter was decreased with ongoing grinding treatment. The aspect ratio of cellulosic fiber was obviously increased with increasing mechanical fibrillation, resulting in the flexible and elongated nature of cellulosic fiber. Moreover, the completely nanofibrillated cellulose with a strong capacity of entanglement was aggregated and twisted, causing a highly entangled fiber network structure. It played an important role in the rheological behavior and stability of cellulosic fiber suspensions.

Rheological properties of cellulose suspension

Steady state viscosity versus shear rate in controlled shear mode of cellulosic fiber suspensions with the different times of grinding treatment are shown in Fig. 3. All curves exhibited the typical shear-thinning behavior. This was because the original fiber network was destroyed, leading to the fiber orientation movement along flow lines upon the shear force, as shown in Fig. 4. Strong evidence of increasing viscosity of suspension was found when the concentration of cellulosic fiber was improved. There was an entangled fiber network structure in the serried fiber suspension. Importantly, it was observed that the mechanical fibrillation leaded to obvious increment of viscosity at the same concentration. For example, at a shear rate of 0.1 s^{-1}, the viscosities of suspensions for A10, A20, and A40 were 5.73 Pa.s, 23.33 Pa.s, and 54.21 Pa.s, respectively. As previous study reported, the viscosity of cellulose suspension was increased as the homogenization treatment (Taheri and Samyn 2016). It is generally accepted that the viscosity of cellulose suspensions obtained by mechanical treatments mainly depends on the strength of the fiber network structure. The large gap of viscosity appeared between the sample A10 and A40, indicating the formation of stronger fiber network structure of completely nanofibrillated cellulose. It was attributed to the strong capacity of entanglement of the long and flexible fiber obtained by mechanical fibrillation.

The oscillatory strain sweep and frequency sweep were measured in order to clarify the viscoelastic behavior and fiber network structure of cellulosic fiber suspensions. Oscillatory strain tests were usually used for studying the linear viscoelastic region. As shown in Fig. 5a-c, linear viscoelastic response to strain-independent of all suspensions were found at low strain region. At this region, the storage modulus ($G^{'}$) was much greater than the loss modulus ($G^{''}$). Once strain exceeded the critical strain, $G^{'}$ decreased rapidly and intersected with $G^{''}$ due to the destroyed fiber network structure, transforming into nonlinear behavior (Nechyporchuk et al. 2016). The oscillatory frequency tests were carried out at the linear viscoelastic region. In order to evaluate the viscoelastic behavior, the value of $G^{'}$ and $G^{''}$ were compared according to the previous report of Li et al. (Li et al. 2015). At low angular frequency, $G^{''} >> G^{'}$ and $\tan \delta > 1$, both $G^{'}$ and $G^{''}$ obviously improved with the increasing angular frequency, suggesting the viscous rheological behavior. On the contrary, $G^{'} > G^{''}$ and $\tan \delta < 1$, the storage modulus was independent of frequency, displaying the gel-like behavior. The viscoelastic modulus of cellulosic fiber suspensions as functions of frequency (ω) and the loss tangent value are shown in Fig. 2d-i. The concentration of cellulosic fiber had a significant effect on the viscoelastic behavior. The cellulosic fiber suspensions presented the typical viscous rheological behavior at low cellulose concentration (0.25% and 0.50%) due to the weak fiber network. The loss tangent value was distinctly decreased with the increased concentration of cellulose, indicating that the phase of suspension was transformed to a strong elastic behavior. For A10 suspensions, the weak elastic behavior was found only in the cellulosic fiber suspension with a concentration of 1.0%, in which $G^{'}$ and $G^{''}$ almost overlapped at low frequency regions, while $G^{'}$ was larger than $G^{''}$ at high frequency regions. Therefore, the phase transition occurred between the cellulose concentration of 0.75–1.0%. In the same way, as the cellulose concentration increased, the phase transition of A20 suspension and A40 suspension happened between the concentration of 0.50–0.75%. But the loss tangent value of A40 suspension was smaller than A20 suspension at the same

concentration, implying the stronger gel-like behavior. Consequently, as the same fiber concentration, the viscoelastic behavior of cellulosic fiber suspensions was dominated by the morphological properties of cellulose. As the mechanical fibrillation increased, the cellulose was completely nanofibrillated, resulting in the individually long and flexible fiber had the strong capacity of entanglement. The completely nanofibrillated cellulose was aggregated and twisted to form an entangled fiber network structure.

The measurements of response time from the retarded strain recovery after creep were measured to investigated the stress-dependent rheological properties. The creep compliance as function of time are shown in Fig. 5a-c. The creep compliance value of cellulosic fiber suspensions was obviously reduced with the increasing of fiber concentration. For example, the maximum creep compliance value of A40 suspensions with the fiber concentration of 0.25%, 0.50%, 0.75%, and 1.0% were 21.27 Pa^{-1}, 2.40 Pa^{-1}, 0.32 Pa^{-1}, and 0.04 Pa^{-1}, respectively. The creep compliance result is the ratio of strain to stress, thus suggesting the deformation in per unit stress (Yuan et al. 2021). More fibers participated in the formation of rigid fiber network that can sustain its stability under the small deformation. Moreover, the mechanical fibrillation had significant effect on the creep compliance and the strain recovery. It was obvious that more times of grinding treatments resulted in lower value of creep compliance at the same concentration. The step wise augment of mechanical fibrillation of A10, A20, and A40 leaded to the maximum creep compliance of suspension of 0.72 Pa^{-1}, 0.14 Pa^{-1}, and 0.04 Pa^{-1}, respectively. The small creep compliance value stands for high capacity of anti-deformation. Thus, the extremely entangled fiber network can maintain the structure and limit fiber orientation movement under the low shear rate as shown in Fig. 4. The strong fiber network structure and stable cellulosic fiber suspension can be obtained by more mechanical fibrillation.

Apparent yield stress is considered as the significant rheological parameter of cellulosic fiber suspensions in the process of production and utilization. It is the minimum stress that drives the cellulose suspension to flow. As shown in Fig. 5d, the apparent yield stress was dramatically increased with the increasing of fiber concentration, suggesting that the suspension with high fiber concentration needs more external stress to break the fiber network structure for driving flow. The morphological properties of cellulose play an important role in the apparent yield stress of cellulosic fiber suspension. At fiber concentration of 1.0%, the yield stress of suspensions for A10, A20, and A40 were 0.35 Pa, 4.3 Pa, and 6.1 Pa, respectively. The apparent yield stress was obviously increased after more mechanical fibrillation. As mentioned above, the long and flexible nanofibrillated cellulose formed the strong fiber network structure which could resist the excess stress.

Figure 5e gives the alteration of dynamic modulus during dynamic time sweeps for dynamic stability of cellulosic fiber suspensions. For A20 and A40 suspensions, when the strain level was at 500%, the original fiber network structure was disrupted immediately, resulting in the viscous fluid behavior. However, at the second strain level of 0.1%, it was clear that the modulus was obviously reduced compared with the initial levels. And the subsequent dynamic modulus could maintain the same level during continuous dynamic time sweeps. It indicated that the cellulosic fiber suspensions obtained by mechanical fibrillation had outstanding dynamic stability and good repeatability, due to the outstanding

self-assembly ability and strong capacity of entanglement of cellulose. However, there was a slight difference of the viscoelastic modulus in the process of destruction and reconstruction of fiber network between A10 and other samples. It suggested that the squashed cellulose could reform a new fiber network structure, but with a weak repetitive stability. This was due to the limited self-assembly ability and capacity of entanglement of the large and rigid squashed cellulose produced by less mechanical fibrillation. Consequently, more mechanical fibrillation could dramatically fibrillated cellulose resulting in the long and flexible nanofibrillated cellulose, which created an extremely entangled fiber network structure.

Figure 2f shows the effect of temperature on the shear viscosity of cellulosic fiber suspensions with different mechanical fibrillation. It was well known that high temperature could introduce energy to disrupt the entangled fiber network structure, improving the fibers to move freely and resulting in the decreased viscosity. As A20 and A40 possessed the highly entangled fiber network structure, their viscosities were marginally decreased as the temperature improved due to the decreased viscosity of water and the slight increment of fiber mobility under high temperature. But the sample of A10 exhibited an obvious decrease of viscosity as the temperature increased. This was because the squashed cellulose had high mobility without the limitation of entangled fibril network structure under high temperature. It indicated that mechanical fibrillation could improve the stability of viscosity of cellulosic fiber suspension under high temperature.

Conclusions

In this work, we investigated the relationships between mechanical fibrillation, morphological properties, and rheological properties of cellulosic fiber. Mechanical fibrillation played a vital role in the morphological properties, thereby exhibiting various rheological behaviors of cellulosic fiber suspensions. The morphological changes of cellulose were the process of “squashed - incompletely nanofibrillated - completely nanofibrillated” with increasing the mechanical fibrillation. The squashed cellulose had a large size, small aspect ratio, and weak capacity of entanglement, resulting in weak fiber network structure. The corresponding suspension exhibited low viscosity, weak anti-deformation capacity, small apparent yield stress, and poor dynamic stability. As mechanical fibrillation increased, the degree of fibrillation was improved. The long and flexible nanofibrillated cellulose had a strong capacity of entanglement and created an entangled fiber network structure, so its suspension exhibited high viscosity, large apparent yield stress, strong elastic gel-like behavior, excellent anti-deformation capacity and dynamic stability. The deep sights in the relationship between morphological properties, fiber network structure and rheological behavior will provide practical guidance on novel rheology-dependent cellulose-based materials.

Declarations

Acknowledgment

This research was financially supported by Characterization and instrument development of cross-scale nanofiber based on microfluidic technology (2020ZD01), National Key R&D Program of China (2017YFB0307902), Natural Science Foundation of Guangdong Province (2019A1515010996) China Postdoctoral Science Foundation (2019TQ0100, BX20200134), the Fundamental Research Funds for the Central Universities (2019MS085 and 2017YFB0307902), and Joint Foundation of the Guangdong Natural Science Foundation for Young Scholar (2020A1515110855).

Conflicts of Interest

The authors declare no conflict of interest.

Availability of data and material

All the data and materials are accessible

Code availability

Not applicable

Authors' contribution

Tianzhong Yuan: Conception, Design, Acquisition, Analysis, Interpretation.

Jinsong Zeng: Drafting, Revising, Correspondence.

Bin Wang: Final approval of the version.

Zheng Cheng: Drafting, Revising.

Kefu Chen: Final approval of the version, Agreement to be accountable for all aspects.

Ethics approval

This article does not contain any studies with human participants or animals performed by any of the authors.

References

1. Abdul Khalil HPS, Davoudpour Y, Islam MN, Mustapha A, Sudesh K, Dungani R, Jawaid M (2014) Production and modification of nanofibrillated cellulose using various mechanical processes: a review. Carbohyd Polym 99:649–665. http://doi.org/10.1016/j.carbpol.2013.08.069
2. Albornoz-Palma G, Betancourt F, Mendonça RT, Chinga-Carrasco G, Pereira M (2020) Relationship between rheological and morphological characteristics of cellulose nanofibrils in dilute dispersions. Carbohyd Polym 230:115588. http://doi.org/10.1016/j.carbpol.2019.115588

3. Alves L, Ferraz E, Lourenço AF, Ferreira PJ, Rasteiro MG, Gamelas JAF (2020) Tuning rheology and aggregation behaviour of tempo-oxidised cellulose nanofibrils aqueous suspensions by addition of different acids. Carbohyd Polym 237:116109. http://doi.org/10.1016/j.carbpol.2020.116109
4. Bai L, Huan S, Xiang W, Rojas OJ (2018) Pickering emulsions by combining cellulose nanofibrils and nanocrystals: phase behavior and depletion stabilization. Green Chemistry 20:1571–1582. http://doi.org/10.1039/C8GC00134K
5. Bian H, Gao Y, Luo J, Jiao L, Wu W, Fang G, Dai H (2019) Lignocellulosic nanofibrils produced using wheat straw and their pulping solid residue: from agricultural waste to cellulose nanomaterials. Waste Manage 91:1–8. http://doi.org/10.1016/j.wasman.2019.04.052
6. Chen J, Huang M, Kong L (2020) Flexible ag/nanocellulose fibers sers substrate and its applications for in-situ hazardous residues detection on food. Appl Surf Sci 533:147454. http://doi.org/10.1016/j.apsusc.2020.147454
7. Chen P, Yu H, Liu Y, Chen W, Wang X, Ouyang M (2013) Concentration effects on the isolation and dynamic rheological behavior of cellulose nanofibers via ultrasonic processing. Cellulose 20:149–157. http://doi.org/10.1007/s10570-012-9829-7
8. Czaikoski A, Da Cunha RL, Menegalli FC (2020) Rheological behavior of cellulose nanofibers from cassava peel obtained by combination of chemical and physical processes. Carbohyd Polym 248:116744. http://doi.org/10.1016/j.carbpol.2020.116744
9. Derakhshandeh B, Hatzikiriakos SG, Bennington CPJ (2010) The apparent yield stress of pulp fiber suspensions. J Rheol 54:1137–1154. http://doi.org/10.1122/1.3473923
10. Dhand AP, Poling-Skutvik R, Osuji CO (2021) Simple production of cellulose nanofibril microcapsules and the rheology of their suspensions. Soft Matter. http://doi.org/10.1039/D1SM00225B
11. Dimic-Misic K, Gane PAC, Paltakari J (2013) Micro- and nanofibrillated cellulose as a rheology modifier additive in cmc-containing pigment-coating formulations. Ind Eng Chem Res 52:16066–16083. http://doi.org/10.1021/ie4028878
12. Dinic J, Sharma V (2020) Power laws dominate shear and extensional rheology response and capillarity-driven pinching dynamics of entangled hydroxyethyl cellulose (hec) solutions. Macromolecules 53:3424–3437. http://doi.org/10.1021/acs.macromol.0c00077
13. Espert M, Wiking L, Salvador A, Sanz T (2020) Reduced-fat spreads based on anhydrous milk fat and cellulose ethers. Food Hydrocolloid 99:105330. http://doi.org/10.1016/j.foodhyd.2019.105330
14. Gómez HC, Serpa A, Velásquez-Cock J, Gañán P, Castro C, Vélez L, Zuluaga R (2016) Vegetable nanocellulose in food science: a review. Food Hydrocolloid 57:178–186. http://doi.org/10.1016/j.foodhyd.2016.01.023
15. Grishkewich N, Mohammed N, Tang J, Tam KC (2017) Recent advances in the application of cellulose nanocrystals. Curr Opin Colloid in 29:32–45. http://doi.org/10.1016/j.cocis.2017.01.005
16. Habibi Y (2014) Key advances in the chemical modification of nanocelluloses. Chem Soc Rev 43:1519–1542. http://doi.org/10.1039/C3CS60204D

17. Heggset EB, Aaen R, Veslum T, Henriksson M, Simon S, Syverud K (2020) Cellulose nanofibrils as rheology modifier in mayonnaise-a pilot scale demonstration. Food Hydrocolloid 108:106084. http://doi.org/10.1016/j.foodhyd.2020.106084
18. Hoeng F, Denneulin A, Reverdy-Bruas N, Krosnicki G, Bras J (2017) Rheology of cellulose nanofibrils/silver nanowires suspension for the production of transparent and conductive electrodes by screen printing. Appl Surf Sci 394:160–168. http://doi.org/10.1016/j.apsusc.2016.10.073
19. Iotti M, Gregersen ØW, Moe S, Lenes M (2011) Rheological studies of microfibrillar cellulose water dispersions. J Polym Environ 19:137–145. http://doi.org/10.1007/s10924-010-0248-2
20. Jiang E, Amiralian N, Maghe M, Laycock B, McFarland E, Fox B, Martin DJ, Annamalai PK (2017) Cellulose nanofibers as rheology modifiers and enhancers of carbonization efficiency in polyacrylonitrile. ACS Sustain Chem Eng 5:3296–3304. http://doi.org/10.1021/acssuschemeng.6b03144
21. Jiang Y, De La Cruz JA, Ding L, Wang B, Feng X, Mao Z, Xu H, Sui X (2020) Rheology of regenerated cellulose suspension and influence of sodium alginate. Int J Biol Macromol 148:811–816. http://doi.org/10.1016/j.ijbiomac.2020.01.172
22. Karato SI, Wu P (1993) Rheology of the upper mantle: a synthesis. Science 260:771–778. http://doi.org/10.1126/science.260.5109.771
23. Karppinen A, Vesterinen A, Saarinen T, Pietikäinen P, Seppälä J (2011) Effect of cationic polymethacrylates on the rheology and flocculation of microfibrillated cellulose. Cellulose 18:1381–1390. http://doi.org/10.1007/s10570-011-9597-9
24. Kedzior SA, Gabriel VA, Dubé MA, Cranston ED (2020) Nanocellulose in emulsions and heterogeneous water-based polymer systems: a review Adv Mater e2002404. http://doi.org/10.1002/adma.202002404
25. Li M, Wu Q, Song K, Lee S, Qing Y, Wu Y (2015) Cellulose nanoparticles: structure–morphology–rheology relationships. ACS Sustain Chem Eng 3:821–832. http://doi.org/10.1021/acssuschemeng.5b00144
26. Li M, Wu Q, Song K, Qing Y, Wu Y (2015) Cellulose nanoparticles as modifiers for rheology and fluid loss in bentonite water-based fluids. ACS Appl Mater Inter 7:5006–5016. http://doi.org/10.1021/acsami.5b00498
27. Lindström T (2017) Aspects on nanofibrillated cellulose (nfc) processing, rheology and nfc-film properties. Curr Opin Colloid in 29:68–75. http://doi.org/10.1016/j.cocis.2017.02.005
28. Mendoza L, Gunawardhana T, Batchelor W, Garnier G (2019) Nanocellulose for gel electrophoresis. J Colloid Interf Sci 540:148–154. http://doi.org/10.1016/j.jcis.2019.01.017
29. Moberg T, Sahlin K, Yao K, Geng S, Westman G, Zhou Q, Oksman K, Rigdahl M (2017) Rheological properties of nanocellulose suspensions: effects of fibril/particle dimensions and surface characteristics. Cellulose 24:2499–2510. http://doi.org/10.1007/s10570-017-1283-0
30. Moon RJ, Martini A, Nairn J, Simonsen J, Youngblood J (2011) Cellulose nanomaterials review: structure, properties and nanocomposites. Chem Soc Rev 40:3941.

http://doi.org/10.1039/c0cs00108b

31. Nechyporchuk O, Belgacem MN, Bras J (2016) Production of cellulose nanofibrils: a review of recent advances. Ind Crop Prod 93:2–25. http://doi.org/10.1016/j.indcrop.2016.02.016
32. Nechyporchuk O, Belgacem MN, Pignon F (2016) Current progress in rheology of cellulose nanofibril suspensions. Biomacromolecules 17:2311–2320. http://doi.org/10.1021/acs.biomac.6b00668
33. Peng J, Calabrese V, Veen SJ, Versluis P, Velikov KP, Venema P, van der Linden E (2018) Rheology and microstructure of dispersions of protein fibrils and cellulose microfibrils. Food Hydrocolloid 82:196–208. http://doi.org/10.1016/j.foodhyd.2018.03.033
34. Phanthong P, Reubroycharoen P, Hao X, Xu G, Abudula A, Guan G (2018) Nanocellulose: extraction and application. Carbon Resources Conversion 1:32–43. http://doi.org/10.1016/j.crcon.2018.05.004
35. Quennouz N, Hashmi SM, Choi HS, Kim JW, Osuji CO (2016) Rheology of cellulose nanofibrils in the presence of surfactants. Soft Matter 12:157–164. http://doi.org/10.1039/C5SM01803J
36. Sun X, Wu Q, Zhang J, Qing Y, Wu Y, Lee S (2017) Rheology, curing temperature and mechanical performance of oil well cement: combined effect of cellulose nanofibers and graphene nano-platelets. Mater Design 114:92–101. http://doi.org/10.1016/j.matdes.2016.10.050
37. Taheri H, Samyn P (2016) Effect of homogenization (microfluidization) process parameters in mechanical production of micro- and nanofibrillated cellulose on its rheological and morphological properties. Cellulose 23:1221–1238. http://doi.org/10.1007/s10570-016-0866-5
38. Tian C, Luo S, She J, Qing Y, Yan N, Wu Y, Liu Z (2019) Cellulose nanofibrils enable flower-like biocl for high-performance photocatalysis under visible-light irradiation. Appl Surf Sci 464:606–615. http://doi.org/10.1016/j.apsusc.2018.09.126
39. Wang W, Mozuch MD, Sabo RC, Kersten P, Zhu JY, Jin Y (2016) Endoglucanase post-milling treatment for producing cellulose nanofibers from bleached eucalyptus fibers by a supermasscolloider. Cellulose 23:1859–1870. http://doi.org/10.1007/s10570-016-0946-6
40. Wang Y, Xie W, Wu D (2020) Rheological properties of magnetorheological suspensions stabilized with nanocelluloses. Carbohyd Polym 231:115776. http://doi.org/10.1016/j.carbpol.2019.115776
41. Xu Y, Atrens A, Stokes JR (2019) Structure and rheology of liquid crystal hydroglass formed in aqueous nanocrystalline cellulose suspensions. J Colloid Interf Sci 555:702–713. http://doi.org/10.1016/j.jcis.2019.08.022
42. Xu Y, Atrens A, Stokes JR (2020) A review of nanocrystalline cellulose suspensions: rheology, liquid crystal ordering and colloidal phase behaviour. Adv Colloid Interfac 275:102076. http://doi.org/10.1016/j.cis.2019.102076
43. Xu Y, Atrens AD, Stokes JR (2017) Rheology and microstructure of aqueous suspensions of nanocrystalline cellulose rods. J Colloid Interf Sci 496:130–140. http://doi.org/10.1016/j.jcis.2017.02.020
44. Yadav C, Saini A, Zhang W, You X, Chauhan I, Mohanty P, Li X (2021) Plant-based nanocellulose: a review of routine and recent preparation methods with current progress in its applications as

rheology modifier and 3d bioprinting. Int J Biol Macromol 166:1586–1616. http://doi.org/10.1016/j.ijbiomac.2020.11.038

45. Yuan T, Zeng J, Wang B, Cheng Z, Chen K (2021) Lignin containing cellulose nanofibers (lcnfs): lignin content-morphology-rheology relationships. Carbohyd Polym 254:117441. http://doi.org/10.1016/j.carbpol.2020.117441
46. Yuan T, Zeng J, Wang B, Cheng Z, Gao W, Xu J, Chen K (2021) Silver nanoparticles immobilized on cellulose nanofibrils for starch-based nanocomposites with high antibacterial, biocompatible, and mechanical properties. Cellulose 28:855–869. http://doi.org/10.1007/s10570-020-03567-y
47. Zhuo X, Liu C, Pan R, Dong X, Li Y (2017) Nanocellulose mechanically isolated fromamorpha fruticosa linn. ACS Sustain Chem Eng 5:4414–4420. http://doi.org/10.1021/acssuschemeng.7b00478

Figures

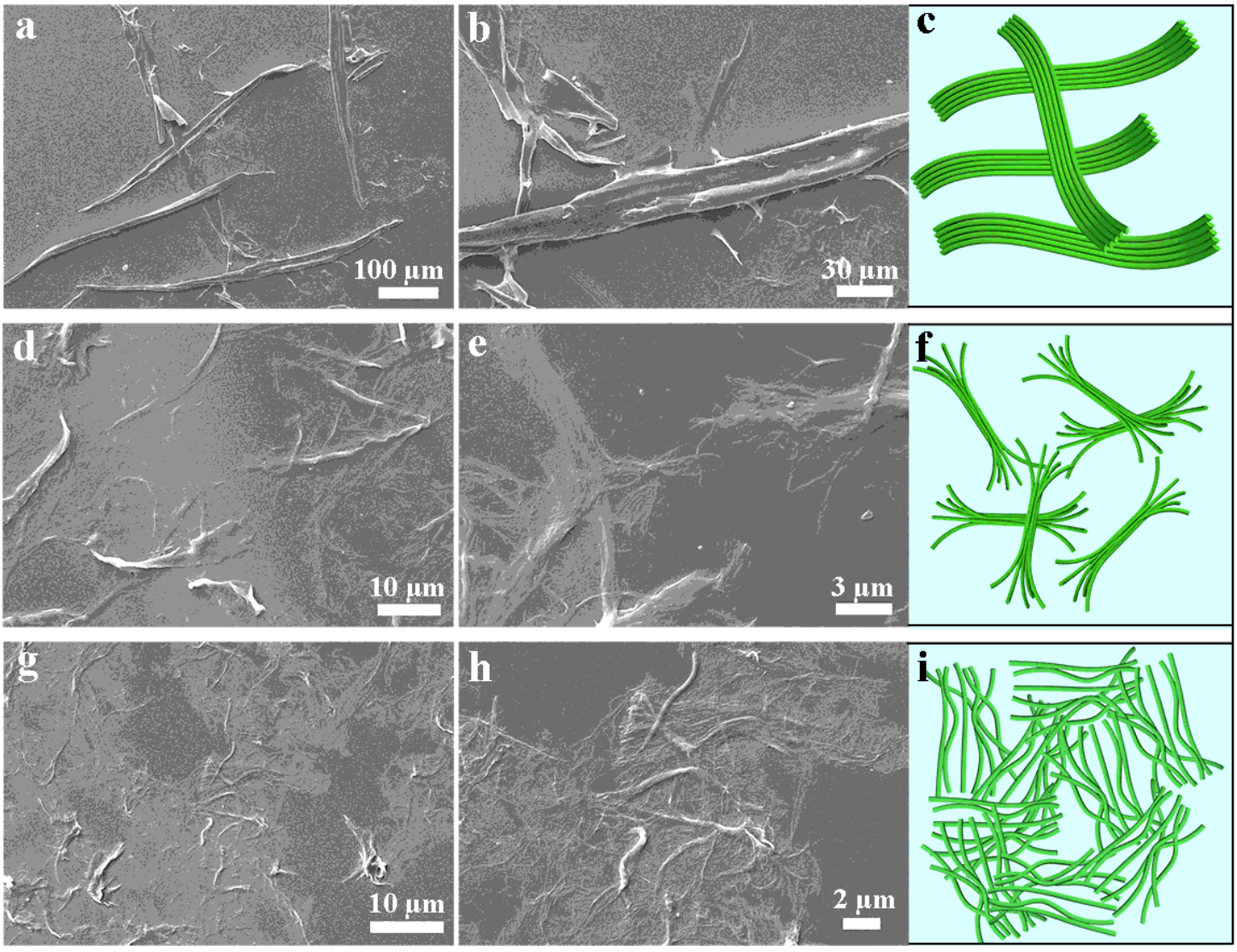

Figure 1

SEM images with different magnifications of A10 (a and b), A20 (d and e), and A40 (g and h). The schematic morphological properties of cellulosic fibers of A10 (c), A20 (f), and A40 (i).

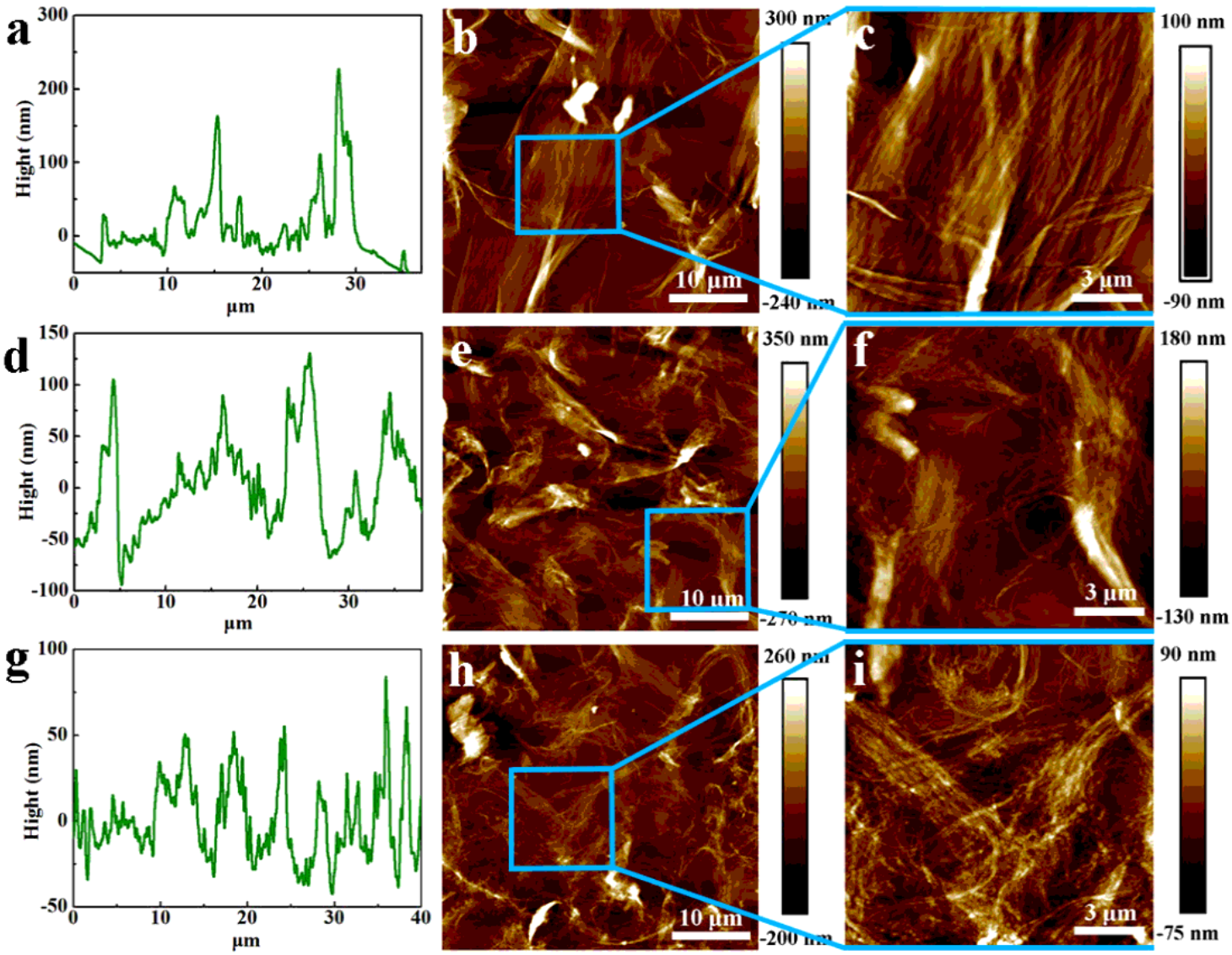

Figure 2

Height profile of cellulosic fiber with different mechanical fibrillation: A10 (a), A20 (d), A40 (g); and AFM image of cellulosic fiber with different mechanical fibrillation: A10 (b and c), A20 (e and f), and A40 (h and i). Rheological properties of cellulose suspension

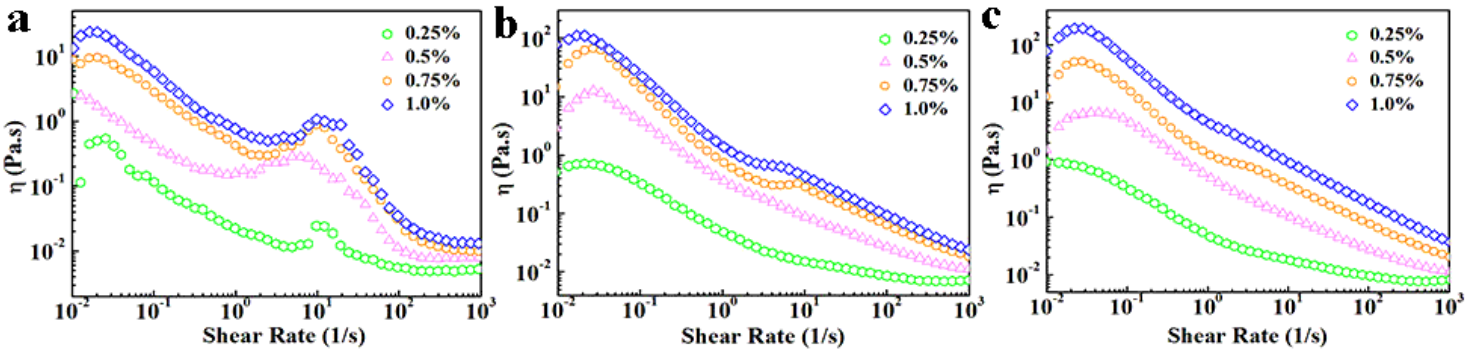

Figure 3

Shear rate versus viscosity plots of cellulosic fiber suspensions of A10 (a), A20 (b), and A40 (c).

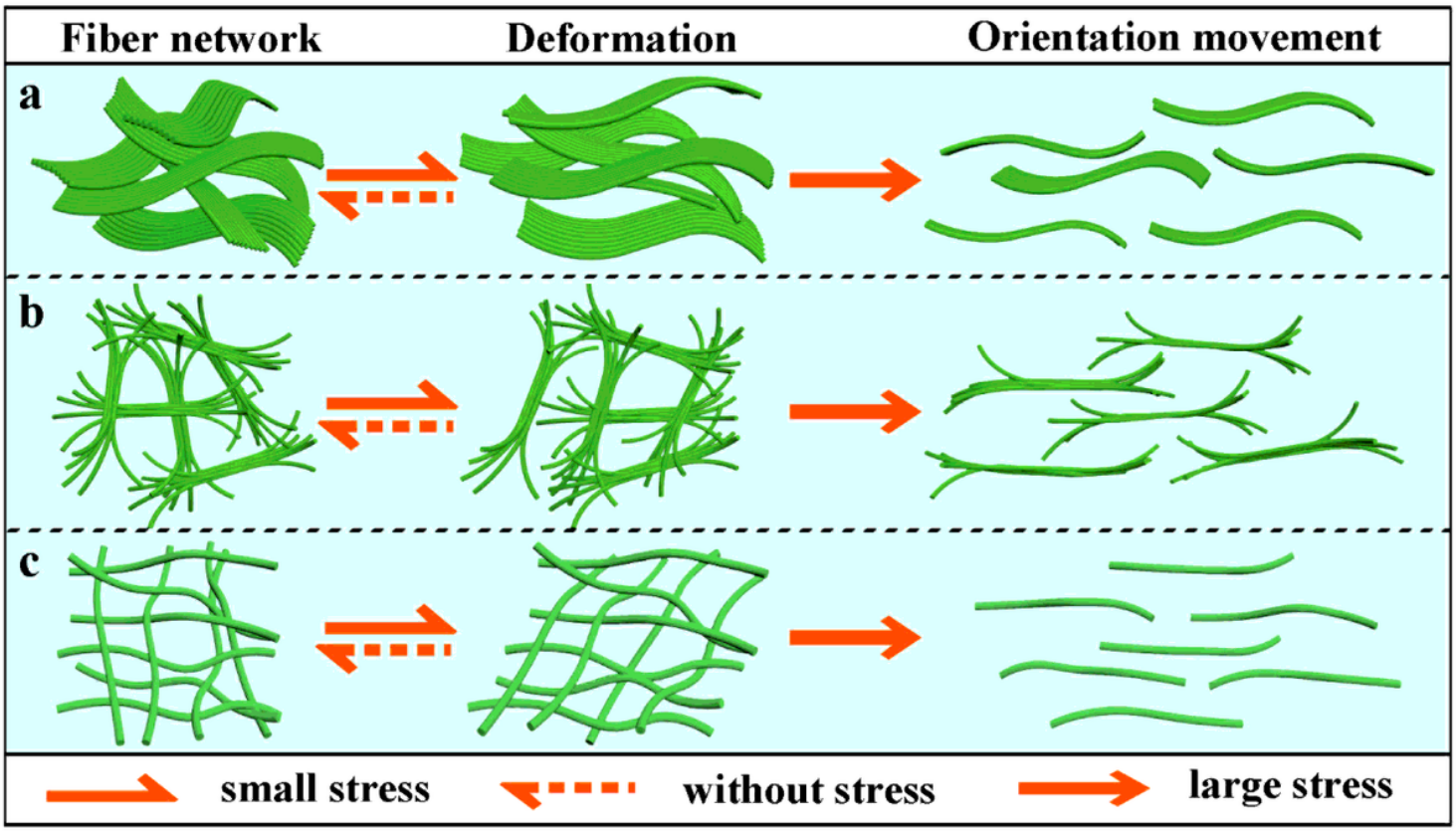

Figure 4

Schematic illustrations of fiber network structure of A10 (a), A20 (b), and A40 (c) during the process of deformation, recovery, and orientation movement.

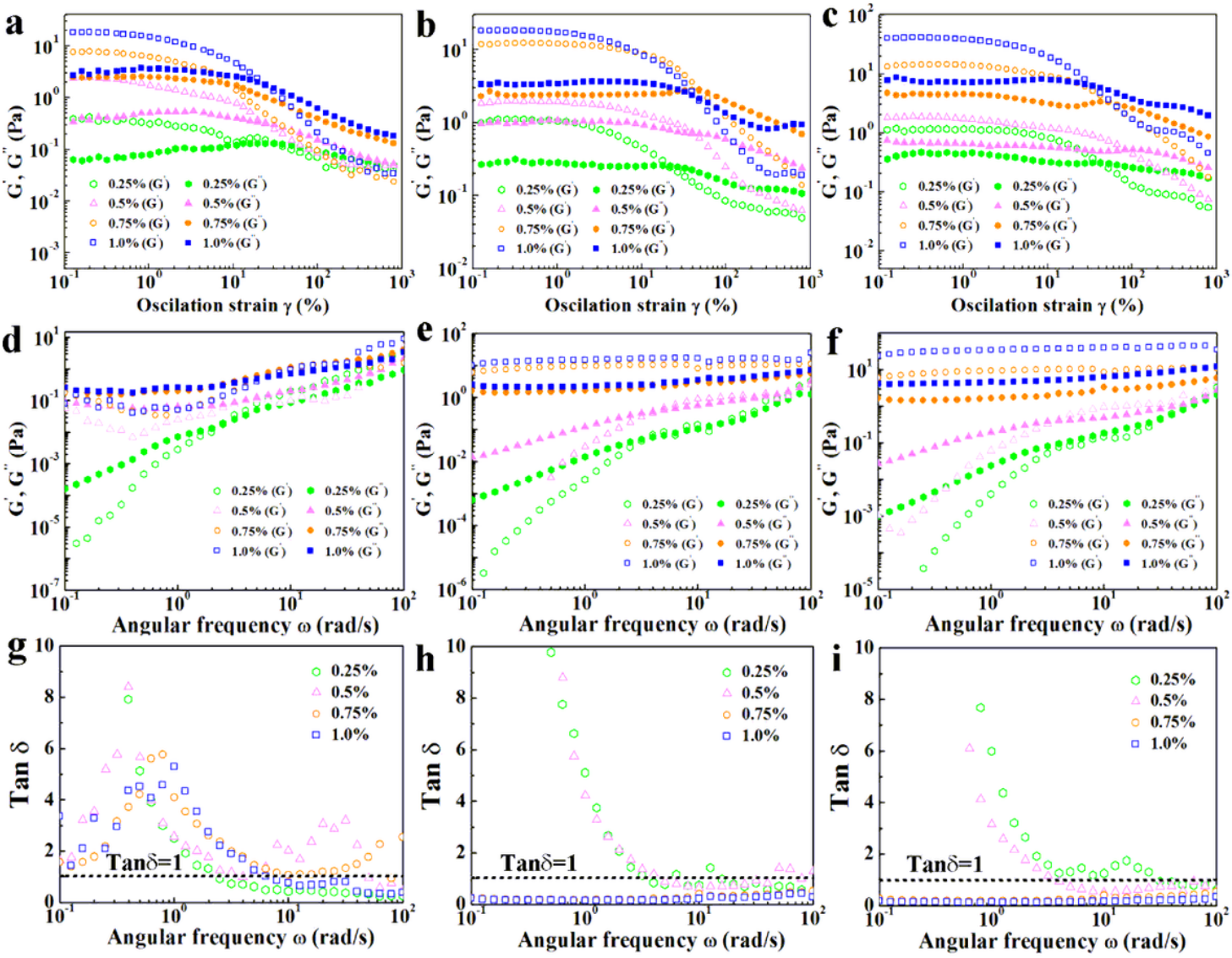

Figure 5

Storage modulus (open symbols) and loss modulus (solid symbols) for cellulosic fiber suspensions of A10 (a), A20 (b), and A40 (c) with different concentration obtained by strain sweeps; the storage modulus (open symbols) and loss modulus (solid symbols) for cellulosic fiber suspensions of A10 (d), A20 (e), and A40 (f) with different concentration obtained by frequency sweeps; the loss tangent cellulosic fiber suspensions of A10 (g), A20 (h), and A40 (i) with different concentration.

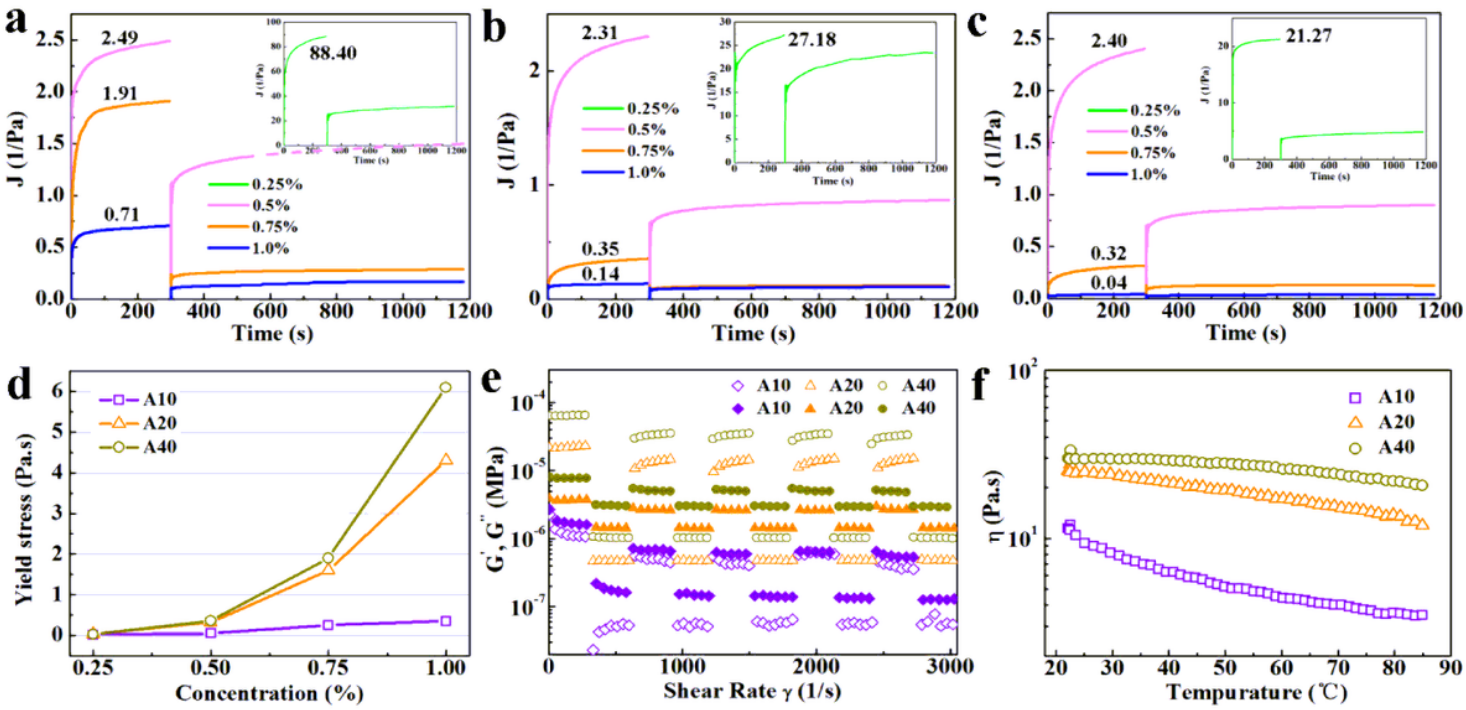

Figure 6

Creep for tcreep = 300s loading stress and strain recovery for trecovery = 900s without stress of cellulosic fiber suspensions of A10 (a), A20 (b), and A40 (c) with different concentration; Apparent yield stress (d) of cellulosic fiber suspensions with different concentration; Storage modulus (open symbols) and loss modulus (solid symbols) as a function of time of cellulosic fiber suspensions (e); The viscosity as function of temperature of cellulosic fiber suspension (f).

Supplementary Files

This is a list of supplementary files associated with this preprint. Click to download.

- SupplementaryMaterial.docx